ELSEVIER

Journal of Alloys and Compounds 446–447 (2007) 575–578

Journal of ALLOYS AND COMPOUNDS

www.elsevier.com/locate/jallcom

Effect of H_2S on hydrogen permeation of $Pd_{60}Cu_{40}$/V–15Ni composite membrane

J.Y. Yang [a,b,*], C. Nishimura [a], M. Komaki [a]

[a] *Hydrogen Purification Materials Group, Fuel Cell Materials Center, National Institute for Materials Science, Sengen 1-2-1, Tsukuba, Ibaraki 305-0047, Japan*

[b] *State Key Laboratory of Materials Processing and Die and Mould Technology, Huazhong University of Science and Technology, 1037 Luoyu Road, Wuhan, Hubei 430074, PR China*

Received 21 September 2006; received in revised form 16 December 2006; accepted 18 December 2006
Available online 27 December 2006

Abstract

Pd–Cu alloy covered V–15Ni composite membranes have been prepared in this work. XRD, SEM and AES analysis were performed to characterize the composite membranes. Hydrogen permeation of the composite membrane under pure hydrogen and mixed gas with H_2S impurity were studied, and the composition and thickness of Pd–Cu overlayers were optimized. It shows that the $Pd_{60}Cu_{40}$/V–15Ni composite membrane has higher permeability than other overlayer compositions. In the temperature range of 573–673 K, the $Pd_{60}Cu_{40}$/V–15Ni composite membrane shows a good resistance to H_2S impurity; when the temperature is lower than 573 K, the effect of H_2S impurity becomes more serious and the hydrogen permeability of $Pd_{60}Cu_{40}$/V–15Ni composite membrane decreases rapidly with increasing of H_2S concentration.

Keywords: Hydrogen permeation; Pd–Cu films; Vanadium nickel alloy; Composite membrane; Hydrogen sulfide

1. Introduction

As a clean and recoverable energy carrier, hydrogen has become an important alternative fuel for solving worldwide energy and environmental crises [1]. Pure hydrogen not only serves as fuel for fuel cells, but is also an important feedstock for many industrial and high-tech applications [2,3]. Currently, there are several methods for preparing pure hydrogen, among them; metallic membrane separation is one of the most cost-effective and promising methods for high purity hydrogen. Pd and its alloys are most extensively used for hydrogen separation, however it is too expensive to use in a large scale [4,5]. To develop new membrane materials with low cost and high performance for hydrogen separation, many efforts have been made in recent years [6]. Several kinds of high permeable materials [7–11] are under development at present. Among them, the V–15Ni alloy, which was developed by Nishimura et al. [8], shows good workability and resistance to hydrogen embrittlement and higher permeability than Pd and Pd alloys. However, V–15Ni membrane is easy to oxidize and not active to hydrogen molecule dissociation; depositing a thin overlayer of Pd or Pd alloys on the V–15Ni membrane to form a composite membrane is proved to be a good solution, and the cost of such composite membranes will be far lower than those of pure Pd or Pd alloys membranes. A lot of research had been done on Pd/V–15Ni and Pd–Ag/V–15Ni composite membranes [12–16] and higher hydrogen permeability than pure Pd and Pd–Ag alloy membranes was obtained. In comparison with Pd and Pd–Ag alloys, Pd–Cu alloys (wt.% Pd > 60) membranes have similar hydrogen permeability [17] with them, and it is cheaper than Pd and Pd–Ag alloys, furthermore, they shows better resistance to poisoning and deactivation by H_2S, the most frequent impurity in hydrogen mixed gas [18,19]. Recently, we did a preliminary work on a Pd–Cu/V–15Ni composite membrane for hydrogen permeation [20,21], as a successive work on hydrogen permeation of Pd–Cu/V–15Ni composite membranes, effect of H_2S on hydrogen permeation properties of the composite membrane will be reported in this paper.

---

[*] Corresponding author. Tel.: +86 27 87540944; fax: +86 27 87556109.
E-mail address: Junyou.Yang@163.com (J.Y. Yang).

0925-8388/$ – see front matter © 2006 Elsevier B.V. All rights reserved.
doi:10.1016/j.jallcom.2006.12.083

2. Experiments

Circular V–15Ni membrane samples with a diameter of 12 mm, which were processed with the same procedures as in previous work [8,9], were used as the substrates for deposition of Pd–Cu overlayer. They were firstly mechanically polished and then chemically polished using a solution with a composition of hydrofluoric acid solution (48 wt.%): nitric acid solution (70 wt.%): lactic acid solution (90 wt.%) = 1:1:1 in volume. After chemical polishing, the substrates are 300 μm in thickness. To minimize oxide and other surface impurity, the chemically polished membrane was further cleaned by fast ion bombardment (FAB) in the FAB chamber for 30 min, and then directly sent into the sputtering chamber for film deposition. Pd–Cu films were prepared in a dc sputtering system with separate Pd and Cu targets (purity of both, 99.99 at.%) in argon atmosphere. To ensure composition homogeneity of the film, the substrate holder could rotate at different speed and the distance between target and substrate is adjustable. Voltage for each target can be varied in the range of 0–600 V. The Pd–Cu films were deposited on each side of the as-prepared V–15Ni substrates under the following sputtering conditions: the base pressure for sputtering was 6.0×10^{-6} Pa, the target–substrate distance and work pressure were set at 60 mm and 1.6 Pa, respectively, and films are deposited at room temperature. The voltage of Pd target was fixed at 340 V while the voltage of Cu target varied between 0 and 600 V to control the overlayer composition. The composition of Pd–Cu films was analyzed using EDX and AES, the thickness of as-sputtered films was measured using FE-SEM.

Hydrogen permeation measurements for the composite membrane were carried out from 423 to 673 K under pure H_2 and a mixed gas of $H_2 + H_2S$, respectively, with an upstream pressure about 40 kPa, using a permeation apparatus described in the previous work [9]. By measuring the hydrogen permeation flux (J), upstream pressure (P_1) and downstream pressure (P_2) at steady state, the hydrogen permeability (Φ) could be determined by the equation: $\Phi = JL(P_1^{1/2} - P_2^{1/2})^{-1}$, where L is the thickness of sample. Usually, P_2 is very small and could be neglected.

3. Results and discussion

As reported in our previous work [21], keeping the voltage of Pd target constant at 340 V, Cu concentration of the overlayer could be expressed as a function of Cu target voltage: x_{Cu} (wt.%) = 0.45 V_{Cu}−138 (V_{Pd} = 340 V, V_{Cu} > 300 V), where V_{Pd} and V_{Cu} are the voltage of Pd and Cu target, respectively, so the composition of Pd–Cu overlayer could be controlled easily by adjusting the voltage of Cu target, hereinafter the overlayer composition is expressed as $Pd_{100-x}Cu_x$, where x refers to weight percent.

Fig. 1 shows the surface morphology of the as-deposited $Pd_{60}Cu_{40}$ film. It can be seen that the film has a very fine microstructure, and it looks very dense and there is no evident pinhole in the film.

An AES depth profile of the $Pd_{60}Cu_{40}$/V–15Ni composite membrane, where the $Pd_{60}Cu_{40}$ overlayer was deposited for 60 s, was shown in Fig. 2, the AES sputtering rate is 20 nm/min. It can be seen that both Pd and Cu intensities show very homogeneous distribution along the thickness direction, and the overlayer thickness could also be evaluated as about 200 nm. The nano-overlayer has a fcc Pd(Cu) solid solution structure [21].

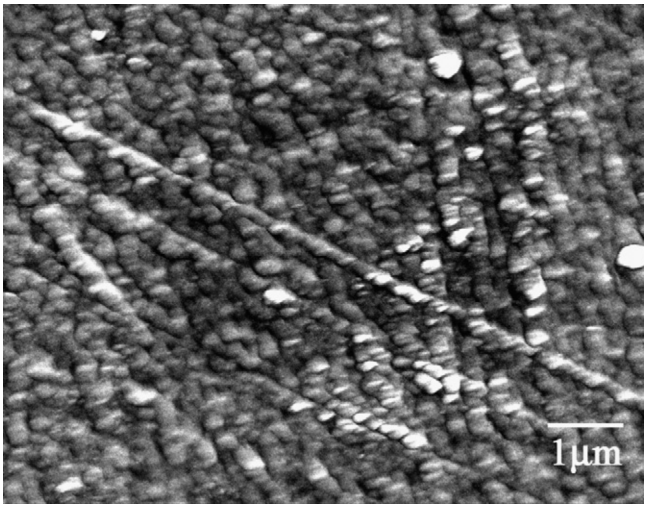

Fig. 1. SEM morphology of the $Pd_{60}Cu_{40}$/V–15Ni composite membrane deposited for 60 s.

For hydrogen permeable composite membrane, thinner and dense overlayer is more preferable because it means less Pd metal. Therefore, thickness control is very important to the Pd–Cu alloy overlayer. To study the relationship between the overlayer thickness and depositing time, we deposited the $Pd_{60}Cu_{40}$ films for different times and measured their thickness with the back scattering electron images of their cross-section and showed the results in Fig. 3. It can be seen that the overlayer thickness shows a linear dependence on depositing time. For V_{Pd} = 340 V and V_{Cu} = 395 V, the depositing rate is about 3.5 nm/s.

Fig. 4 shows the relationship between the hydrogen permeability of the composite membranes and their overlayer composition. It can be seen that the hydrogen permeability increases with Cu content until 40 wt.% Cu, and then it decreases rapidly with Cu content increasing. The $Pd_{60}Cu_{40}$/V–15Ni composite membrane presents the highest hydrogen permeability. The overlayer with Cu content higher than 40 wt.% is not suitable for hydrogen permeation.

Hydrogen permeability of the $Pd_{60}Cu_{40}$/V–15Ni composite membrane with different overlayer thickness that corresponds to deposition time as 30, 60, 90 and 120 s, respectively, was shown in Fig. 5. The hydrogen permeability of the composite membrane first increases when the deposition time increases from 30 to 60 s,

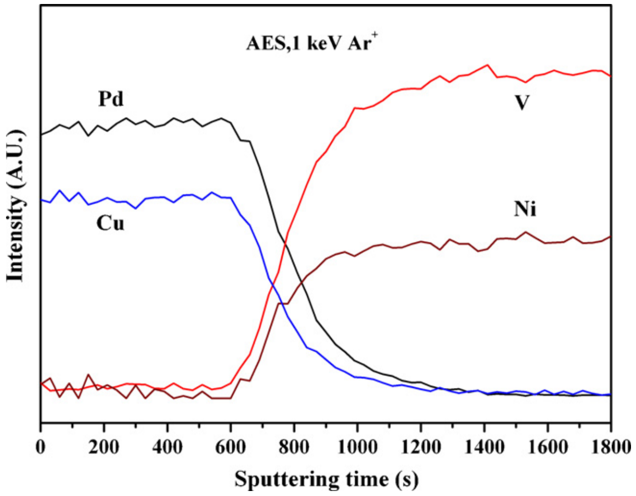

Fig. 2. AES depth profile of the $Pd_{60}Cu_{40}$/V–15Ni composite membrane with the $Pd_{60}Cu_{40}$ overlayer deposited for 60 s (AES sputtering rate: 20 nm/min.).

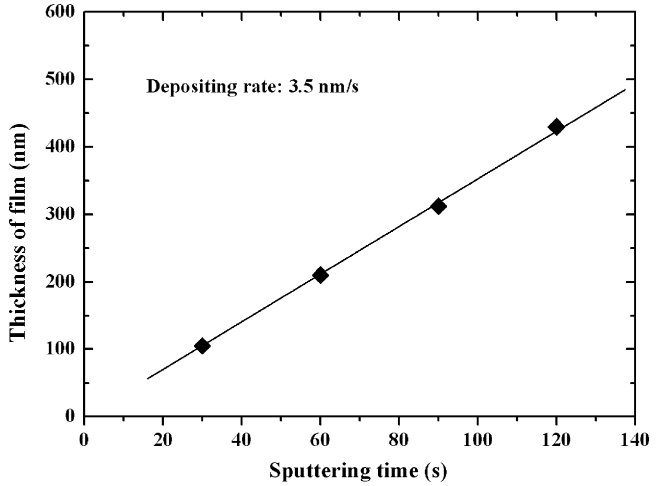

Fig. 3. Variation of the $Pd_{60}Cu_{40}$ overlayer thickness with depositing time (V_{Pd} = 340 V, V_{Cu} = 395 V).

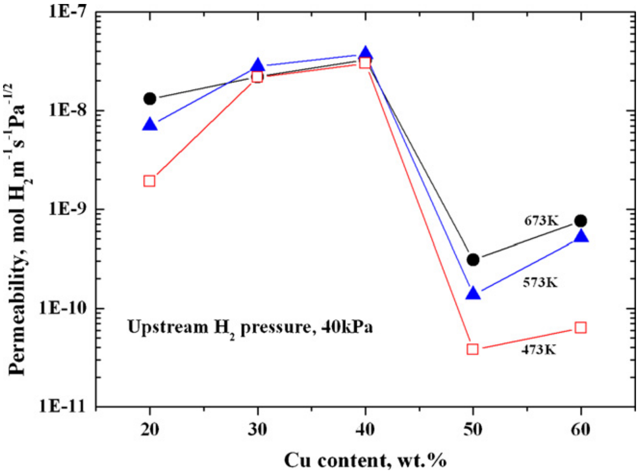

Fig. 4. Variation of the hydrogen permeability of the composite membrane with the Cu content of the overlayer.

and the 60 s sample which corresponds to an overlayer thickness about 200 nm has the highest hydrogen permeability among all the samples, and the maximum permeability was obtained at 573 K as 3.72×10^{-8} mol H_2 m^{-1} s^{-1} $Pa^{-1/2}$. As for the composite membrane deposited for 30 s, the overlayer was very thin (about 100 nm) and its coverage to the V–15Ni substrate was also not so complete, SEM observation shows there are some sparse sites in the overlayer, so it is understandable that it has lower permeability than that of the composite membrane deposited for 60 s. Further increasing the overlayer thickness, the hydrogen permeability decreases. Considering the thickness of the composite membrane is about 300 μm, hydrogen diffusion across the composite membrane should be the rate-controlling step. Ignoring the interface or surface effect, according to the Barrie's model [22], the hydrogen permeability for dense composite membrane could be expressed as:

$$\frac{L_1+L_2+L_3}{\Phi}=\frac{L_1}{\Phi_1}+\frac{L_2}{\Phi_2}+\frac{L_3}{\Phi_3},$$

where L_i denotes the thickness of the ith layer, and Φ_i and Φ mean the hydrogen permeability of the ith layer and the composite membrane respectively. Considering that the hydrogen permeability of the $Pd_{60}Cu_{40}$/V–15Ni composite membrane is quite larger than that of single $Pd_{60}Cu_{40}$ membrane [20], it is reasonable to deduce that the hydrogen permeability of V–15Ni membrane (Φ_2) is larger than that of $Pd_{60}Cu_{40}$ membrane (Φ_1). Therefore, hydrogen permeability of the $Pd_{60}Cu_{40}$/V–15Ni composite membrane (Φ) decreases with increasing the thickness of the $Pd_{60}Cu_{40}$ overlayer (L_1) could be qualitatively explained by Barrie model. Further research is under way.

To study the effect of H_2S impurity on hydrogen permeability of $Pd_{60}Cu_{40}$/V–15Ni composite membrane, the $Pd_{60}Cu_{40}$/V–15Ni composite membrane with $Pd_{60}Cu_{40}$ overlayer thickness of 200 nm was measured in a mixed gases of $H_2 + H_2S$ with different H_2S concentration, and the results were shown in Fig. 6. It can be seen that $Pd_{60}Cu_{40}$/V–15Ni com-

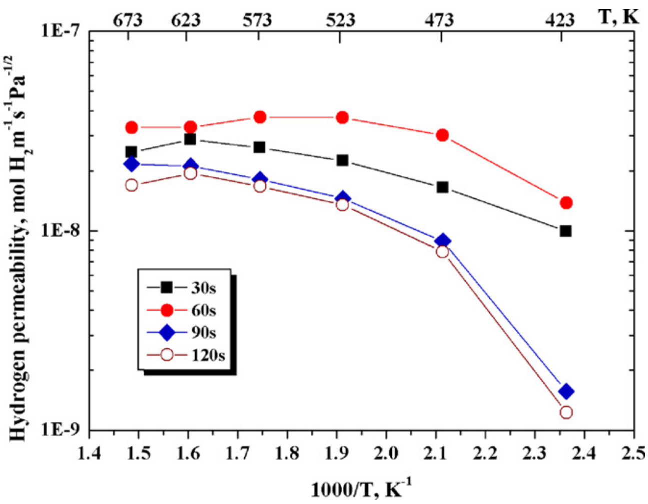

Fig. 5. Variation of the hydrogen permeability of composite membrane with the deposition time of the $Pd_{60}Cu_{40}$ overlayer.

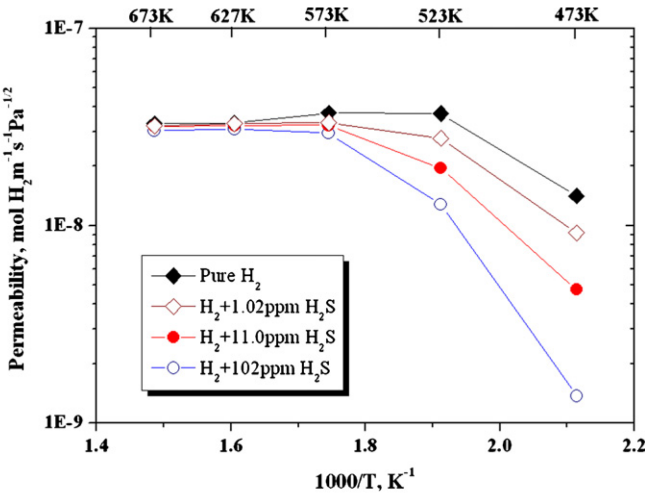

Fig. 6. Variation of the hydrogen permeability of the $Pd_{60}Cu_{40}$/V–15Ni composite membrane with the H_2S content of mixed gas (the overlayer thickness: 200 nm).

posite membrane shows a good resistance to H_2S impurity in the temperature range of 573–673 K; when the temperature is lower than 573 K, the effect of H_2S impurity becomes more serious and the hydrogen permeability of $Pd_{60}Cu_{40}$/V–15Ni composite membrane decreases rapidly with the increasing of H_2S concentration. What should be pointed out is, all data in Fig. 6 were obtained with the same sample measured sequentially in different mixed gases. That is to say, the composite membrane could recover its hydrogen permeability in high temperature (573–673 K), even if it was degraded by H_2S at low temperature (473–573) in the previous measurement. Therefore, the permeability degradation by H_2S in low temperature should not be attributed to physical destruction to the composite membrane, and the increasing surface adsorption of H_2S to the membrane in low temperature, which lowers the hydrogen solubility of the membrane should the main reason.

4. Conclusions

Pd–Cu alloy covered V–15Ni composite membranes have been prepared in this work. XRD, SEM and AES analysis were performed to characterize the composite membranes. Hydrogen permeation of the composite membrane under pure hydrogen and mixed gas with H_2S impurity were studied, and the composition and thickness of Pd–Cu overlayers were optimized. It shows that the $Pd_{60}Cu_{40}$/V–15Ni composite membrane has higher permeability than other overlayer compositions. In the temperature range of 573–673 K, $Pd_{60}Cu_{40}$/V–15Ni composite membrane shows a good resistance to H_2S impurity; when the temperature is lower than 573 K, the effect of H_2S impurity becomes more serious and the hydrogen permeability of $Pd_{60}Cu_{40}$/V–15Ni composite membrane decreases rapidly with the increasing of H_2S concentration.

References

[1] M. Conte, A. Iacobazzi, M. Ronchetti, R. Vellone, J. Power Sources 100 (2001) 171.

[2] B.D. Mcnicol, D.A.J. Rand, K.R. Williams, J. Power Sources 100 (2001) 47.

[3] M.O.S. Dantas, E. Galeazzo, H.E.M. Peres, F.J. Ramirez-Fernandez, A. Errachid, Sens. Actuators A: Phys. 115 (2004) 608–616.

[4] J. O'Brien, R. Hughes, J. Hisek, Surf. Coat. Technol. 142/144 (2001) 253.

[5] T.S. Moss, N.M. Peachey, R.C. Snow, R.C. Dye, Int. J. Hydrogen Energy 23 (2) (1998) 99.

[6] S. Hara, S. Sakaki, N. Itoh, H.-M. Kimura, K. Asami, A. Inoue, J. Membr. Sci. 164 (2000) 289.

[7] T.S. Moss, N.M. Peachey, R.C. Snow, R.C. Dye, Int. J. Hydrogen Energy 23 (1998) 99.

[8] C. Nishimura, M. Komaki, S. Hwang, M. Amano, J. Alloys Compd. 330/332 (2002) 902.

[9] C. Nishimura, M. Komaki, M. Amano, Trans. Mater. Res. Soc. Jpn. B18 (1994) 1273.

[10] W. Luo, K. Ishikawa, K. Aoki, J. Alloys Compd. 407 (1/2) (2006) 115–117.

[11] K. Ishikawa, T. Takano, T. Matsuda, K. Aoki, Appl. Phys. Lett. 87 (8) (2005) 081906.

[12] Y. Zhang, T. Ozaki, M. Komaki, C. Nishimura, J. Membr. Sci. 224 (2003) 81–91.

[13] Y. Zhang, T. Ozaki, M. Komaki, C. Nishimura, J. Alloys Compd. 356/357 (2003) 553–556.

[14] Y. Zhang, T. Ozaki, M. Komaki, C. Nishimura, J. Membr. Sci. 246 (2005) 173–180.

[15] T. Ozaki, Y. Zhang, M. Komaki, C. Nishimura, Int. J. Hydrogen Energy 28 (2003) 297–302.

[16] T. Ozaki, Y. Zhang, M. Komaki, C. Nishimura, Int. J. Hydrogen Energy 28 (2003) 1229–1235.

[17] D.L. McKinley, US Patent 3,439,474.

[18] D.L. McKinley, US Patent 3,350,845.

[19] B.D. Morreale, M.V. Ciocco, B.H. Howard, R.P. Killmeyer, A.V. Cugini, R.M. Enick, J. Membr. Sci. 241 (2004) 219–224.

[20] J.Y. Yang, C. Nishimura, M. Komaki, J. Membr. Sci. 282 (2006) 337–341.

[21] J.Y. Yang, C. Nishimura, M. Komaki, J. Alloys Compd. 431 (2007) 180–184.

[22] J.A. Barrie, J.D. Levine, A.S. Michaels, P. Wong, Trans. Faraday Soc. 59 (1963) 869.